

# Random Anisotropy Magnet at Finite Temperature

Dmitry A. Garanin and Eugene M. Chudnovsky

*Physics Department, Herbert H. Lehman College and Graduate School, The City University of New York,  
250 Bedford Park Boulevard West, Bronx, New York 10468-1589, USA*

(Dated: January 3, 2022)

We present finite-temperature Monte Carlo studies of a 2D random-anisotropy magnet on lattices containing one million spins. The correlated spin-glass state predicted by analytical theories is reproduced in simulations, as are the field-cooled and zero-field-cooled magnetization curves observed in experiments. The orientations of lattice spins begin to freeze when temperature is lowered. The freezing transition is due to the energy barriers generated by the random anisotropy rather than due to random interactions in conventional spin-glasses. We describe freezing by introducing the time-dependent spin-glass order parameter  $q$  and the spin-melting time  $\tau_M$  defined via  $q = \tau_M/t$  above freezing, where  $t$  is the time of the experiment represented by the number of Monte Carlo steps.

## I. INTRODUCTION

Amorphous and nanocrystalline ferromagnets have multiple technological applications due to their remarkable magnetic softness<sup>1</sup>. Many of such systems are characterized by ferromagnetic exchange and random local magnetic anisotropy. They received the name of random-anisotropy (RA) ferromagnets. Their static properties have been intensively studied in the past, see, e.g., Refs. 2–4 and references therein. Recently, it has been shown that RA magnets can also be excellent broadband absorbers of microwave radiation<sup>5</sup>.

Theoretical research on RA magnets received strong initial boost from a seminal work of Imry and Ma<sup>6</sup> who argued that random on-site field of strength  $h$ , no matter how weak, destroys ferromagnetic order exponentially fast beyond the distance  $R_f$  that scales as  $(J/h)^{2/(4-d)}$ , where  $J$  is the exchange constant and  $d = 1, 2, 3$  is the dimensionality of the system. This gave rise to the concept of Imry-Ma (IM) domains of average size  $R_f$ , representing a system in which local direction of magnetization wanders smoothly on a scale  $R_f$ , resulting in a zero net magnetization of a large system. Although random anisotropy of strength  $D_R$  is different from the random field, it does generate random effective field at the lattice site, which makes plausible the picture of IM domains of size  $R_f \sim (J/D_R)^{2/(4-d)}$  (in lattice units) in that case, too. This magnetic state received the name of the correlated spin glass (CSG)<sup>7,9</sup>.

The CSG theory explained many features of amorphous magnets observed in experiments. Conceptually similar models were developed for arrays of magnetic bubbles<sup>10</sup>, vortex lattices in superconductors<sup>11,12</sup>, charge-density waves<sup>13–15</sup>, liquid crystals<sup>16</sup>, and He-3 in aerogel<sup>17,18</sup> and on corrugated graphene<sup>19</sup>. Later on, the validity of the concept of IM domains was questioned by people who applied the renormalization group theory and replica symmetry breaking methods to the RA model and to the equivalent model of pinned flux lattices in superconductors, see, e.g., Refs. 20,21 and references therein. The Bragg-glass phase characterized by the power-law decay of correlations instead of exponential decay was

proposed, but that prediction was never confirmed by any experiment on magnetic systems.

Another criticism of the IM concept came from its neglect of metastable states<sup>22–24</sup>. It was found numerically that the RA magnets exhibited metastability and history dependence<sup>25,26</sup>, although they do break into IM domains of size predicted by theory if one begins with a fully disordered initial state. It was demonstrated that the relation between the number of spin components and dimensionality of space in the random-field model determines whether the model possesses topological defects, and that the latter is crucial for preservation or decay of the long-range correlations<sup>27–29</sup>.

The RA model turned out to be more challenging than the random-field model. Its exact ground state, spin-spin correlation functions, and classification of topological defects has never been established with certainty despite the significance of RA magnets for applications. Previous analytical work on small lattices, accompanied by Monte Carlo studies, that assumed thermal equilibrium<sup>30–33</sup>, could not describe time-dependent behavior and hysteresis observed in real systems. The hysteresis curve and scaling of coercivity arising from the presence of topological defects in a 3D RA model have been studied numerically in Ref. 4. Scaling arguments were developed that helped understand numerical results.

In this article, with the help of the Monte Carlo technique, we address temporal behavior of RA systems as it is usually done for spin glasses. In particular, we study melting of spin states, that has been seldom investigated theoretically so far. We study the evolution (in terms of Monte Carlo steps) of the RA magnet at different temperatures, starting with the quenched state with a random orientation of spins. This kind of numerical experiment mimics preparation of an amorphous magnet from a disordered paramagnetic state by a melt spinning technique<sup>1</sup>. It helps to answer a long-standing question<sup>34</sup> whether on lowering temperature the RA magnet undergoes freezing of correlated spin groups due to energy barriers created by the local magnetic anisotropy or it exhibits a spin-glass transition due to interaction between correlated spin groups.

Theoretical<sup>35</sup> and experimental<sup>36</sup> studies of that problem so far have addressed systems with large RA compared to the exchange, when individual spins behave similar to single-domain magnetic particles and extended ferromagnetic correlations are absent. Here we study the less obvious limit of a soft magnet in which the RA of the order of the exchange or smaller. It is the case of the CSG with extended ferromagnetic correlations and large magnetic susceptibility.

To study spin correlations in the CSG one needs a large system. The power of modern computers is better suited for that task than it was in the past. Still the 3D case requires impractically large computational times, so we stick to a 2D system of one million spins. The paper is organized as follows. The model and properties of the CSG that follow from the IM argument are discussed in Section II. The freezing parameter and melting time that describe physical properties of the system, together with formulas for magnetization and susceptibility, are introduced in Section III. Our numerical method is described in Section IV. Numerical results on field-cooled and zero-field-cooled magnetization curves are presented in Section V-A. The computed temperature dependence of the freezing parameter and the melting time is given in Section V-B. Results on the magnetization and susceptibility are included in Section V-C. The final Section VI contains discussion of the nature of the observed freezing transition.

## II. THE MODEL

We consider the model of a classical random-anisotropy (RA) ferromagnet on a lattice

$$\mathcal{H} = -\frac{1}{2} \sum_{ij} J_{ij} \mathbf{s}_i \cdot \mathbf{s}_j - \frac{D_R}{2} \sum_i (\mathbf{n}_i \cdot \mathbf{s}_i)^2 - \mathbf{H} \cdot \sum_i \mathbf{s}_i. \quad (1)$$

Here  $J_{ij}$  is the nearest-neighbor coupling of the classical spin vectors  $|\mathbf{s}_i| = 1$  with the coupling constant  $J > 0$ ,  $D_R$  is the RA constant,  $\mathbf{n}_i$  are randomly oriented easy-axis vectors, and  $\mathbf{H}$  is the external field in the energy units. This model shares many features with spin glasses. At low temperatures for  $H = 0$ , spins tend to locally order in the directions of the locally predominant orientation of the anisotropy axis. For  $D_R/J \lesssim 1$  there is a strong short-range order as the ferromagnetic correlation radius<sup>2</sup>

$$R_f \sim a \left( \frac{J}{D_R} \right)^{2/(4-d)} \quad (2)$$

becomes much larger than the lattice spacing  $a$ . There is a numerical factor of about 10 in this formula, see the estimations below Eq. (18). At low temperatures, the magnetic structure consists of large correlated regions in which spins point in the direction of the predominant anisotropy that is random. Such correlated regions can

be called ‘‘Imry-Ma domains’’ (IM domains), although there are no domain walls between them. The correlation radius is especially large in three dimensions,  $d = 3$ . The result for  $R_f$  above can be obtained with the help of the Imry-Ma argument. Suppose the spins are correlated within the distance  $R_f$ . Averaging the RA energy over this region gives the energy

$$E_{RA} \sim -D_R \left( \frac{a}{R_f} \right)^{d/2} \quad (3)$$

per spin for  $a \ll R_f$ . The exchange energy per spin due to the change of the spin field at the distance  $R_f$  is

$$E_{ex} \sim J \left( \frac{a}{R_f} \right)^2. \quad (4)$$

Minimizing the total energy  $E_{tot} = E_{RA} + E_{ex}$  with respect to  $R_f$  yields Eq. (2). For this  $R_f$ , both anisotropy and exchange energies have the same order of magnitude,  $|E_{RA}| \sim E_{ex}$ . This picture assumes that the spins within IM domains are directed along the anisotropy axis averaged over the IM domain.

One can estimate the zero-field zero-temperature susceptibility of the RA magnet as follows.<sup>8,9</sup> If a small uniform field  $H$  is applied, the spins deviate from the dominant-anisotropy direction by a small angle  $\delta\theta$ , that results in the energy change  $\delta E \sim -H\delta\theta + |E_{RA}|(\delta\theta)^2$ . Minimizing this energy with respect to  $\delta\theta$  and using  $|E_{RA}| \sim E_{ex}$ , for the susceptibility in the energy units  $\chi \sim \delta\theta/H$  one obtains

$$\chi = \frac{k}{J} \left( \frac{R_f}{a} \right)^2. \quad (5)$$

where  $k$  is a factor of order unity. The latter depends on the exact form of the spin-spin correlation function. In 2D this factor also contains logarithmic dependence on  $R_f$ . At  $R_f \gg a$  the susceptibility is large, which explains magnetic softness of RA magnets.

As it was mentioned above, the correlated bunches of spins (IM domains) tend to orient themselves in the two possible directions along the predominant anisotropy axis. The energy barrier  $\Delta U$  between these orientations can be estimated as  $\Delta U \sim E_{RA}$ , Eq. (3). Using Eq. (2), one obtains

$$\Delta U \sim D_R \left( \frac{J}{D_R} \right)^{d/(4-d)} = J \left( \frac{D_R}{J} \right)^{\frac{2(2-d)}{4-d}}. \quad (6)$$

In particular,

$$\Delta U \sim J \begin{cases} \left( \frac{D_R}{J} \right)^{2/3}, & d = 1 \\ 1, & d = 2 \\ \left( \frac{J}{D_R} \right)^2, & d = 3. \end{cases} \quad (7)$$

Bunches of spins of the size  $R_f$  that flip over the barrier are not independent but interacting with their neighbors

via the exchange. The interaction energy can be estimated assuming that the distance between the neighboring regions of correlated spins is  $R_f$ , so that the overlap volume is  $R_f^d$ . The interaction energy then has the same form as the exchange energy in the IM argument:

$$E_{int} \sim J \left( \frac{a}{R_f} \right)^2 \left( \frac{R_f}{a} \right)^d = J \left( \frac{R_f}{a} \right)^{d-2} \sim \Delta U. \quad (8)$$

That is, flipping bunches of correlated spins are strongly coupled. Thus the RA magnet has a similarity with an ensemble of interacting magnetic particles with a random anisotropy. However, this analogy is incomplete as IM domains are not real domains and the boundaries between these “particles” are washed out. The fact that the interaction between IM domains is comparable with their effective anisotropy energy makes the situation more complicated. Some of IM domains can be directed along their effective anisotropy axes while some cannot because of the interaction with their neighbors. There should be many different ways to minimize the energy with different sets of “lucky” and “unlucky” IM domains.

The time required to overcome the collective energy barrier for a large number of correlated spins should be very long, so that in the intermediate temperature range the system does not come to equilibrium during sustainable simulation times. At higher temperatures, transitions between different states are faster and the system reaches the full (global) equilibrium. At lower temperatures, spin bunches cannot overcome energy barriers at all. Here, the local equilibrium near one of the many local energy minima of the system is established relatively fast.

In finite-size systems with linear size  $L$ , the results above are valid for  $R_f \lesssim L$ . The value of the random anisotropy at which  $R_f \sim L$  can be estimated as

$$D_R \sim D_R^* = J \left( \frac{a}{L} \right)^{(4-d)/2}. \quad (9)$$

For  $D_R \lesssim D_R^*$  the barrier can be estimated as

$$\Delta U \sim D_R \left( \frac{L}{a} \right)^{d/2} \quad (10)$$

that must be smaller than the value for the infinite system. Upon increasing  $L$ , the barrier approaches its limiting value from below.

### III. THE SPIN-GLASS ORDER PARAMETER AND OTHER COMPUTABLE QUANTITIES

The indicator of the glassy transition is freezing described by the time autocorrelation function averaged over all  $N$  spins:

$$K(\tau) = \frac{1}{N} \sum_{i=1}^N \mathbf{s}_i(t) \cdot \mathbf{s}_i(t + \tau). \quad (11)$$

If the system is at global or local equilibrium, the result does not depend on the time  $t$ . However, in the intermediate temperature interval the system evolves in the direction of equilibrium but cannot reach it during the observation (simulation) time, thus the result also depends on  $t$ . In the glassy state, the spins are frozen and do not deviate much from their initial positions, so that  $K(\tau)$  is finite at large  $\tau$ . Above the glassy transition, spins are fluctuating wildly, so that  $K(\tau) \rightarrow 0$  at large  $\tau$ . For large systems, computation of  $K(\tau)$  is prohibitive as it requires keeping all spin configurations in memory over a long time interval.

The SG order parameter based on the temporal evolution of spins can be defined as

$$q = \frac{1}{N} \sum_{i=1}^N \langle \mathbf{s}_i \rangle_t \cdot \langle \mathbf{s}_i \rangle_t, \quad (12)$$

where

$$\langle \mathbf{s}_i \rangle_t \equiv \frac{1}{t_{\max}} \int_0^{t_{\max}} dt \mathbf{s}_i(t) \quad (13)$$

is the time average over a long time interval. In spin glasses below the freezing point,  $q \rightarrow \text{const}$  for  $t_{\max} \rightarrow \infty$ . This definition is similar to Eq. (1.4) of Ref.<sup>34</sup>. Instead of the time averaging or ensemble averaging we use averaging over statistical samples generated by the Monte Carlo process. Averaging over realizations of the RA was done for smaller systems but it was found that it is better to consider larger systems without this averaging as large systems self-average.

Above the freezing point, the glassy CF  $K(\tau)$  asymptotically vanishes and one can rewrite  $q$  as

$$q \cong \frac{\tau_M}{t_{\max}}, \quad \tau_M \equiv \int_{-\infty}^{\infty} d\tau K(\tau), \quad (14)$$

where  $\tau_M$  is melting time. If there is a true SG transition on temperature, then melting time should diverge on approaching it from above. Studying the coefficient in the asymptotic  $1/t_{\max}$  form of the glassy order parameter  $q$  above freezing could yield the value of the freezing temperature.

One can also compute the autocorrelation function of the average spin (magnetization)

$$\mathbf{m} = \frac{1}{N} \sum_i \mathbf{s}_i \quad (15)$$

that is defined by

$$C(\tau) = \mathbf{m}(t) \cdot \mathbf{m}(t + \tau), \quad (16)$$

In simulations on finite-size systems  $C(\tau)$  is non-zero and can be used to monitor freezing. Unlike  $K(\tau)$ , it can be computed for large systems and large time intervals.

The value of the equal-time correlation function  $C(0) = m^2$  is nonzero in finite-size systems even in the absence of long-range order due to short-range correlations. One has

$$m^2 = \frac{1}{N^2} \sum_{i,j} \mathbf{s}_i \cdot \mathbf{s}_j = \frac{1}{N} \sum_j \langle \mathbf{s}_i \cdot \mathbf{s}_{i+j} \rangle \Rightarrow \frac{1}{N} \int_0^\infty \frac{d^d r}{a^d} G(r), \quad (17)$$

where  $G(r)$  is the spatial correlation function and  $d$  is the dimensionality of the space. As the RA magnet has lots of metastable local energy minima,  $G(r)$  depends on the initial conditions and on the details of the energy minimization routine. In 2D for  $G(r) = \exp[-(r/R_f)^p]$  one obtains

$$m^2 = K_p \frac{\pi R_f^2}{N a^2} \quad \Rightarrow \quad \frac{R_f}{a} = m \sqrt{\frac{N}{\pi K_p}}, \quad (18)$$

where  $K_1 = 2$  and  $K_2 = 1$ .

Having estimated  $R_f$ , one can find the number of IM domains  $N_{IM}$  in the system of size used in the numerical work. In 2D with linear sizes  $L_x$  and  $L_y$  one has  $N_{IM} = L_x L_y / (\pi R_f^2)$ . In particular, for a system with  $N = 300 \times 340 = 102000$  spins and  $D_R/J = 0.3$ , energy minimization at  $T = 0$  starting from a random spin state yields  $m \approx 0.21$ , and with  $p = 2$  one obtains  $R_f/a \approx 37.8$  and  $N_{IM} \approx 23$ . For  $D_R/J = 1$ , one obtains  $m \approx 0.074$  and  $R_f/a \approx 13.3$  that yields  $N_{IM} \approx 183$ . For the ratio of the  $R_f$  values one obtains  $R_f^{(D_R=0.3)}/R_f^{(D_R=1)} \approx 2.84$  that is close to the value 3.33 given by Eq. (2).

One can compute the linear static susceptibility differentiating the statistical expression for the average magnetization value  $\langle \mathbf{m} \rangle$ . The differential susceptibility per spin has the form

$$\chi_{\alpha\alpha} = \frac{\partial \langle m_\alpha \rangle}{\partial H_\alpha} = \frac{N}{T} \left( \langle m_\alpha^2 \rangle - \langle m_\alpha \rangle^2 \right), \quad (19)$$

where the average is taken over the statistical ensemble and  $\alpha = x, y, z$ . Within the Monte Carlo method, the average is taken over the statistical sample generated by the Monte Carlo process. The symmetrized form of the susceptibility in zero field is given by

$$\chi = \frac{N}{3T} \left( \langle \mathbf{m} \cdot \mathbf{m} \rangle - \langle \mathbf{m} \rangle \cdot \langle \mathbf{m} \rangle \right), \quad (20)$$

where  $\langle \mathbf{m} \cdot \mathbf{m} \rangle = \langle m^2 \rangle$ . Whereas the number of spins  $N$  is very large, the difference of the terms in brackets can be very small below freezing, so that the result for a large system does not essentially depend on  $N$ . Unlike the magnetization value  $\langle \mathbf{m} \rangle$  that for a large system can be computed using only one system's state, i.e., without averaging,  $\langle \mathbf{m} \rangle \Rightarrow \mathbf{m}$ , computing  $\chi$  requires averaging over different states of the statistical ensemble. With only one state taken into account,  $\chi$  vanishes. Above the freezing temperature in zero field, one has  $\langle \mathbf{m} \rangle = 0$ , so that only the first term in the susceptibility formula

contributes. In the frozen state, the two terms are close to each other and their difference is small. For this reason, there is a lot of numerical noise in this formula. In the intermediate temperature range the system does not reach equilibrium during the simulation time, so that Eq. (20) becomes questionable as it was obtained under the assumption of equilibrium using the statistical ensemble. The fact that the system does not come to equilibrium is another source of the noise in the simulation results for  $\chi$ . In different simulations, the system is getting stuck in one of the infinite number of energy valleys of its phase space that are characterized by different values of  $\langle \mathbf{m} \rangle$ . However, even in this intermediate region the formula gives plausible results and should be correct at least qualitatively. Using  $\chi_{\alpha\alpha} = \partial \langle m_\alpha \rangle / \partial H_\alpha$  is not much better as the result depends on the time allowed for the system to relax. At high and low temperatures Eq. (20) is correct as either global or local equilibrium is reached.

#### IV. THE NUMERICAL METHOD

Computation of the static properties of RA magnets at  $T > 0$  could be done using real dynamics<sup>39</sup> or Monte Carlo. The latter is much faster and is the way to go. However, as different states of the RA magnet are separated by energy barriers and spins are fluctuating as large correlated groups, there is a very slow relaxation near and below the freezing point, creating a computational challenge. To speed-up the relaxation in simulations, one has to combine the Metropolis Monte Carlo updates that work as slow diffusion in the phase space of the system with overrelaxation updates that simulate conservative dynamics allowing to quickly explore the hypersurfaces of constant energy. For systems with single-site anisotropy, the straightforward overrelaxation routine, rotating the spins by  $180^\circ$  around the effective field, leads to the energy decrease and thus is not working properly.

To beat this problem, we have developed a *thermalized overrelaxation* routine. Here, the spins are rotated by  $180^\circ$  around the different-site part of the effective field (e.g., around the exchange field). As the result, the energy increases or decreases due to the RA. To compensate for this, the rotation is accepted or rejected using the Metropolis criterion, same as in the Monte Carlo updates. In our simulations, for each spin update we used the Metropolis Monte Carlo with the probability  $\alpha = 0.1$  and thermalized overrelaxation with the probability  $1 - \alpha$ . The thermodynamic consistency of this method has been checked by computing the dynamical spin temperature  $T_S$  given by Eq. (9) of Ref.<sup>37</sup>. The values of  $T_S$  were in a good accordance with the set temperature  $T$ .

To minimize the energy of the system at  $T = 0$ , we used the straightforward overrelaxation routine mentioned above that for the systems with uniaxial single-site anisotropy leads to the energy decrease. This routine provides a fast convergence. If in the initial state of the system all spins are collinear, then upon relaxation the

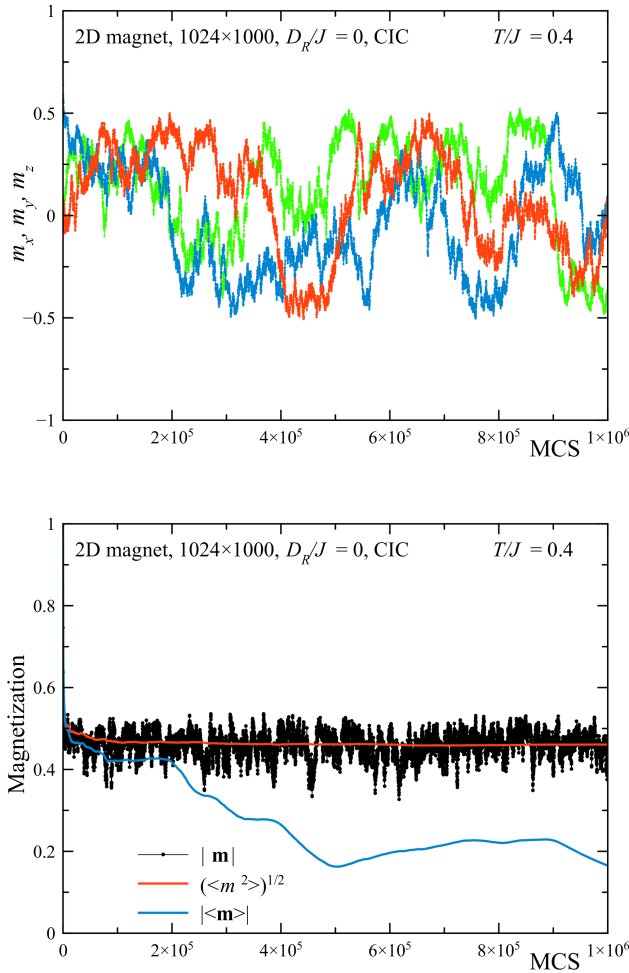


Figure 1: Pure 2D Heisenberg ferromagnetic model. Upper panel: Evolution of the magnetization components. Lower panel: Magnetization, root-mean-square magnetization, and its running average.

system becomes only partially disordered with a significant residual magnetization  $m$ . If the initial state of the system is random, the relaxed state is random, too, with  $m$  being rather small. Most of the simulations were done with the random initial conditions (RIC).

In the computation of the dependence of the SG order parameter  $q$  on  $t_{\max}$ , Eq. (12), we used summation over Monte Carlo steps (MCS) i.e., system updates, instead of the integration over time. That is, instead of Eq. (13) we used

$$\langle \mathbf{s}_i \rangle \equiv \frac{1}{\text{MCS}} \sum_{n=1}^{\text{MCS}} \mathbf{s}_i(n), \quad (21)$$

where  $n$  labels the states generated by the Monte Carlo process. The asymptotic formula for  $q$  above freezing

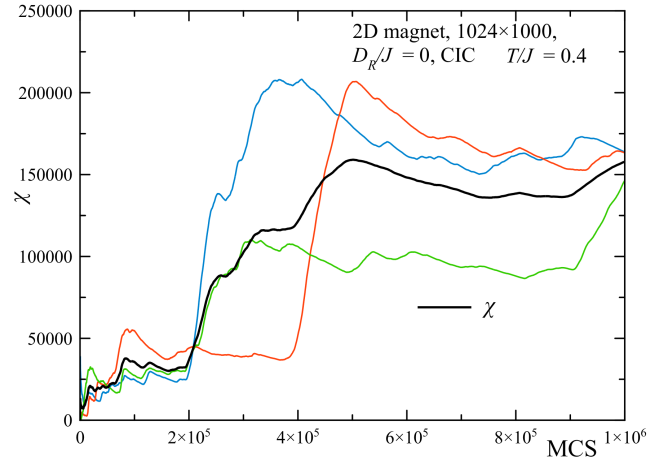


Figure 2: Susceptibility vs simulation time in MCS for the pure 2D Heisenberg ferromagnetic model.

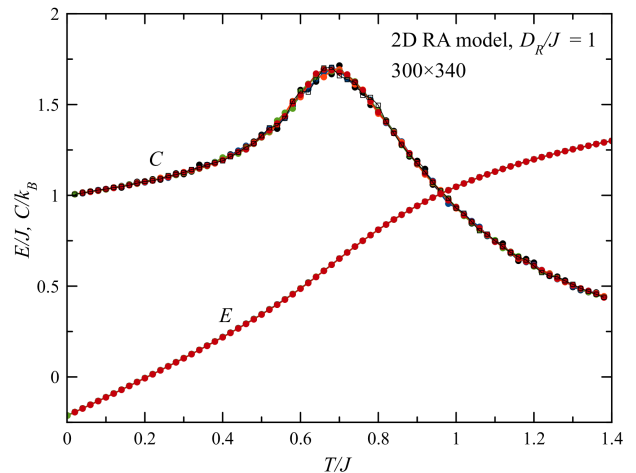


Figure 3: Energy and heat capacity of the 2D RA model.

becomes

$$q \cong \frac{\tau_M}{\text{MCS}}, \quad \tau_M = \sum_{n=-\infty}^{\infty} K(n). \quad (22)$$

Here, the melting time  $\tau_M$  is measured in Monte Carlo steps. While the latter are not related to the time in any simple way, still  $\tau_M$  gives an idea if freezing in the system.

The simulations were done on large 2D systems, typically  $1024 \times 1000$  spins, with periodic boundary conditions. The very large system size is needed as the system of many spins behaves as that of a much smaller number of IM domains. In particular, for  $D_R/J = 1$  the system of  $10^5$  spins is too small and shows large fluctuations. To reduce fluctuations, one can either perform repeated measurements on such systems or simulate a larger system. The latter is preferred.

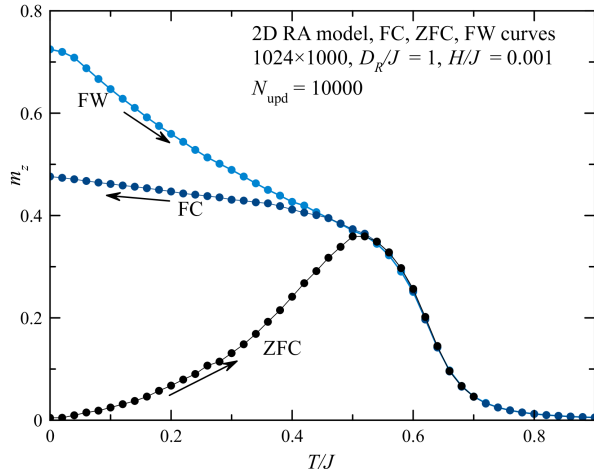


Figure 4: FC, ZFC, and FW curves for a 2D RA model with  $10^6$  spins.

Usually, in Monte Carlo simulations the system is first equilibrated and then measurements of the equilibrium properties are performed. For the RA magnet, the equilibration is extremely long, and around the freezing temperature the system does not come to equilibrium at all after one million MCS that is about our limit for  $10^6$  spins. Thus we resorted to performing a fixed number of MCS for each temperature. Our first attempts included stepwise lowering  $T$  performing from ten to twenty thousand MCS for each temperature point. However, such simulation duration proved to be too short, and increasing it in the cycle over the temperatures would result in exceedingly long computation. Therefore, long simulations, up to  $10^6$  MCS, for select temperature values have been performed, each time starting from quenched states obtained by energy minimization starting from random spin states. Each of these simulations required several days.

As the computing software, Wolfram Mathematica with compilation and parallelization was used. Most of computations were performed on our Dell Precision workstation having 20 CPU cores from which 16 cores were used by Mathematica.

## V. TESTING THE NUMERICAL METHOD ON THE PURE 2D MAGNET

First, we test the numerical method on the pure 2D Heisenberg ferromagnetic model. In this case, the thermalized overrelaxation degenerates to the regular overrelaxation as it conserves energy. There is no phase transition on temperature in this model but a strong short-range order with exponentially large magnetic susceptibility and exponentially long correlation length establishes with lowering temperature in the infinite system. This happens around  $T/J = 0.7$  where the heat capac-

ity has a maximum. In simulations on finite-size systems, further lowering the temperature quickly results in the correlation length exceeding the system size  $L$ , and the system behaves as an ordered magnetic particle. In this regime, the susceptibility is not exponentially large but still huge:  $\chi = N \langle m^2 \rangle / (3T)$ . The results of a single simulation of the pure 2D Heisenberg ferromagnetic model at  $T/J = 0.4$  are shown in Figs. 1 and IV. The equilibrium value of the root-mean-square magnetization  $\langle m^2 \rangle^{1/2}$  stabilizes quickly enough with increasing the number of system updates MCS, as can be seen in the lower panel of Fig. 1). However, computing the linear susceptibility  $\chi$  using Eq. (20) for the system of one million spins requires about a million of system updates, see Fig. IV. Such a long simulation is required to average out the system's magnetization vector  $\mathbf{m}$  that contributes to the second term in Eq. (20). The slow evolution of the components of  $\mathbf{m}$  is shown in the upper panel of Fig. 1. After one million of system updates one obtains  $\chi J = 157838$  that is almost as large as the “magnetic-particle” value defined just above with  $N = 1024 \times 1000$ ,  $\sqrt{\langle m^2 \rangle} = 0.46$ , and  $T/J = 0.4$  that is  $\chi J = 180565$ .

One also can check what becomes the freezing parameter  $q$  of Eq. (12) for the pure system. Theoretically, one expects  $q = 0$  at any  $T > 0$ . However, for a system of  $10^6$  spins at  $T/J = 0.4$  one needs to perform hundreds of thousands MCS to see that the system is not frozen. The dependence of  $q$  on the number of MCS performed is added to Fig. 8 below. These simulations of the pure system show that the problem is computationally involved. In the presence of random anisotropy it becomes harder because of even longer relaxation due to thermally-activated barrier crossing by large groups of correlated spins.

## VI. NUMERICAL RESULTS

### A. FC-ZFC-FW curves

Figure 4 shows the result for the FC, ZFC, and FW curves in a 2D RA model with a million spins and the RA strength  $D_R/J = 1$ . Here a very weak field is applied along  $z$  axis and  $m_z \equiv \langle s_{i,z} \rangle$  was measured. The ZFC curve was obtained by first minimizing the system's energy starting from a random orientation of spins at  $T = 0$  and  $H = 0$ , then applying the field  $H$  and gradual warming the system. The FC curve was obtained by gradual cooling the system from a high temperature to  $T = 0$  in the presence of the field. Finally, the field-warmed (FW) curve was obtained by first minimizing the system's energy in the applied field starting from the state with all spins directed along  $z$  axis and then gradually warming the system. For each temperature point, 10000 system updates were performed. One can see that the ZFC curve merges with the other two curves at  $T/J \simeq 0.53$  that can be interpreted as spin-glass transition or freezing temper-

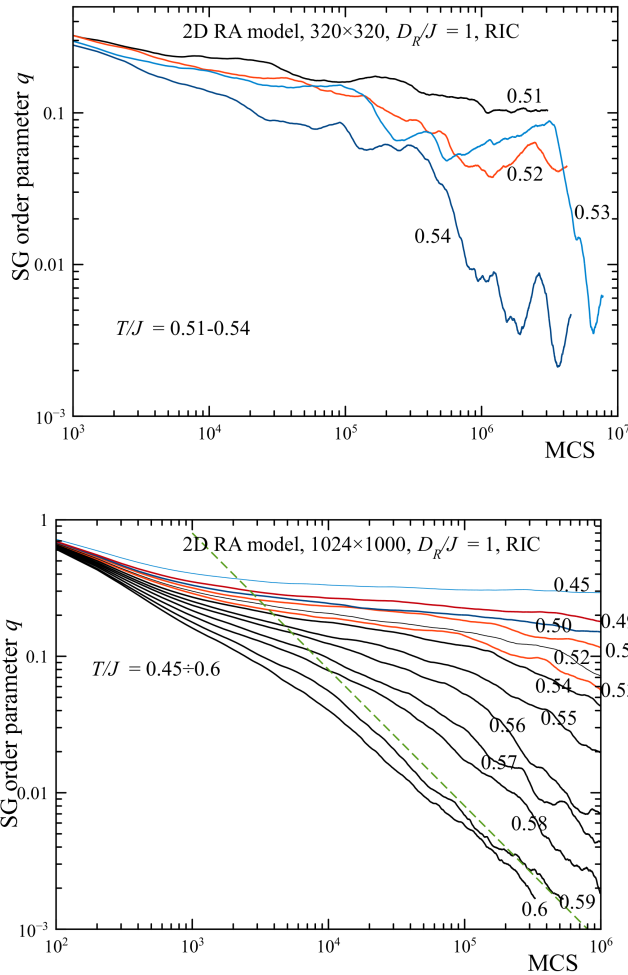


Figure 5: The dependence of the SG order parameter on the number of Monte Carlo steps in log-log scale. Upper panel: a smaller system of  $10^5$  spins. Lower panel: the system of  $10^6$  spins. The dashed line is the asymptote  $q = \tau_M / \text{MCS}$  for  $T/J = 0.59$ .

ature  $T_{SG}$ . The estimated magnetic susceptibility near freezing is huge,  $\chi = m_z / H \simeq 400$ . This is unlike that in the conventional spin glasses with a random exchange. Each curve was obtained by averaging over three different runs. For a system of  $10^5$  spins fluctuations are much stronger, so that a more extensive averaging over runs is needed.

## B. Spin-glass order parameter and melting time

Then, we have performed a long annealing, up to  $10^6$  MCS, of the system at different temperatures after the energy minimization (quenching) starting from random initial conditions. Each of these simulations took several days, so they had to be done one-by-one rather than in a cycle. Each simulation run used its own realization of

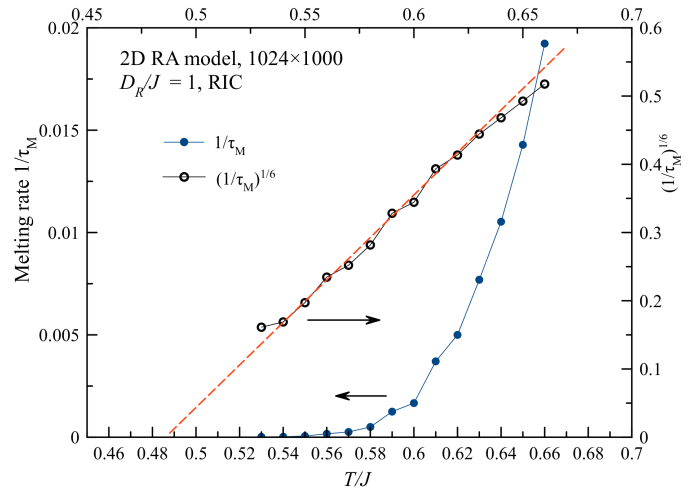


Figure 6: Melting rate above freezing – natural and power-law representations.

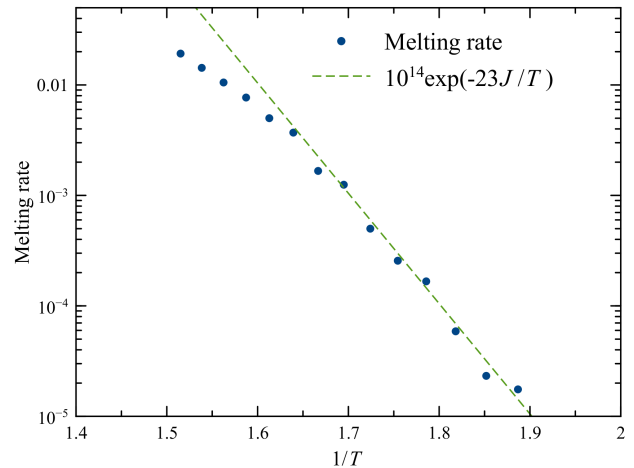


Figure 7: Melting rate above freezing – Arrhenius representation.

the RA and its own random initial spin state. The results of each run were the dependences of  $q$  and the components of the average spin  $\mathbf{m}$ , Eq. (15), vs the number of MCS. From the  $\mathbf{m}$  data, the susceptibility components, Eq. (19) and the symmetrized susceptibility, Eq. (20) were derived.

The dependence of the SG order parameter  $q$  of Eq. (12) on the number of MCS near the freezing temperature for a smaller system of  $10^5$  spins is shown in the upper panel of Fig. 5. One can see that this size is too small, as the system behaves as that of a much fewer number of entities and fluctuations are too strong. For  $T/J = 0.53$  at  $\text{MCS} = 3 \times 10^6$  most of the system's  $10^5$  spins suddenly change their direction that leads to a sharp decrease of  $q$ . A really large system should not behave like this. One has either to perform an extensive

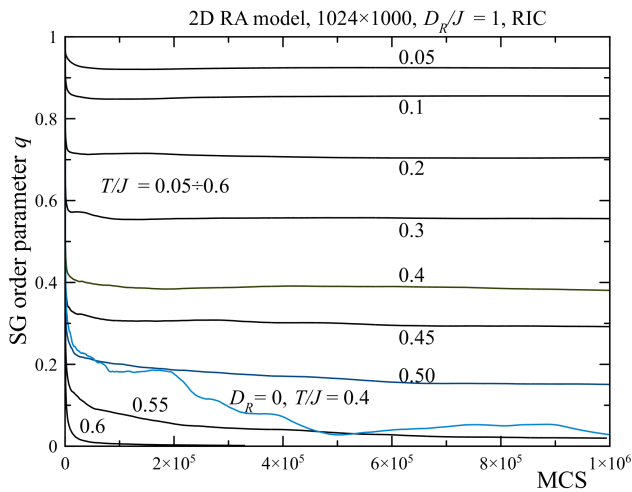


Figure 8: The dependence of the SG order parameter on the number of Monte Carlo steps in linear scale at different temperatures.

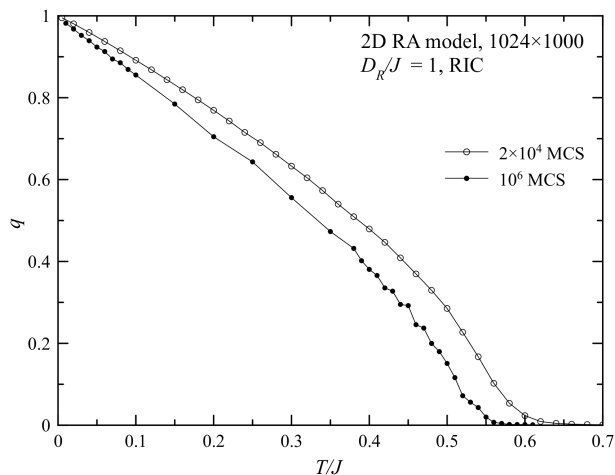


Figure 9: Asymptotic values of the spin-glass order parameter  $q$  at different temperatures. The curve with open circles was obtained by gradually lowering the temperature making  $2 \times 10^4$  MCS for each  $T$  value. The curve with filled circles was obtained by making  $10^6$  MCS at each  $T$  value one by one for different RA realizations.

averaging over runs of take a larger system that is preferable. The data for  $10^6$  spins in the lower panel of Fig. 5 are much smoother and show the asymptotic power-law dependence  $q = \tau_M/\text{MCS}$  above the freezing point, in accordance with Eq. (14).

Fitting the dependence of the SG order parameter with  $q = \tau_M/\text{MCS}$  one can extract the melting time  $\tau_M$ . The latter becomes very large when the system freezes. If there is true phase transition at some freezing temperature  $T_f$ , one can expect a power-law divergence  $\tau_M \propto (T - T_f)^{-\gamma}$ . The results for the melting

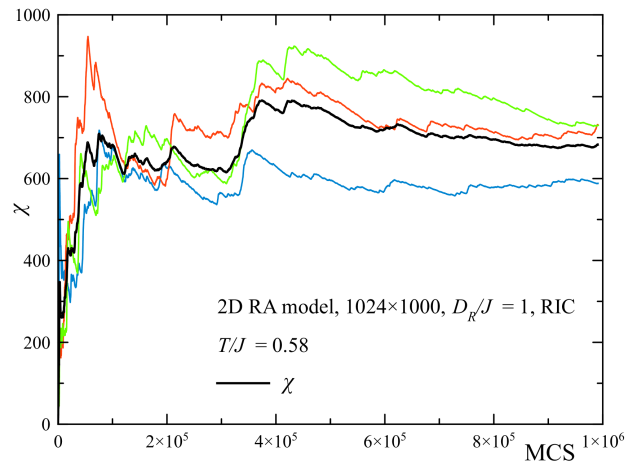
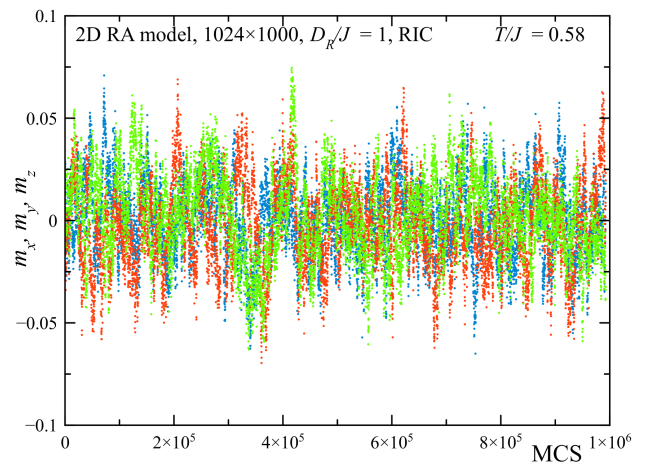


Figure 10: Simulation above the freezing point,  $T/J = 0.58$ . Upper panel: evolution of the magnetization components. Lower panel: dependence of the susceptibility components (colored curves) and the symmetrized susceptibility (black curve) on the number of MCS done.

rate  $1/\tau_M$  are shown in Fig. 6. The temperature dependence of  $1/\tau_M^{1/6}$  is a straight line that suggests  $\gamma = 6$  and  $T_f/J \simeq 0.49$ . The power 6 is too high to be credible while the freezing temperature is rather low and difficult to approach from above because of too slow relaxation requiring exorbitant computing times.

Another way to fit the results for the melting time is using the Arrhenius temperature dependence  $\tau_M \propto \exp(\Delta U/T)$ . The corresponding data representation shown in Fig. 7 yields the barrier value  $\Delta U = 23J$ . Theoretically, Eq. (7) yields  $\Delta U \sim J$  for  $d = 2$  but there can be a large numerical factor in  $\Delta U$ . At larger temperatures, one can see expected deviations from the Arrhenius law (as well as deviations from the power law in Fig. 6). This interpretation implies that there is no phase transition and freezing is a gradual process.

Another argument in favor of a gradual freez-

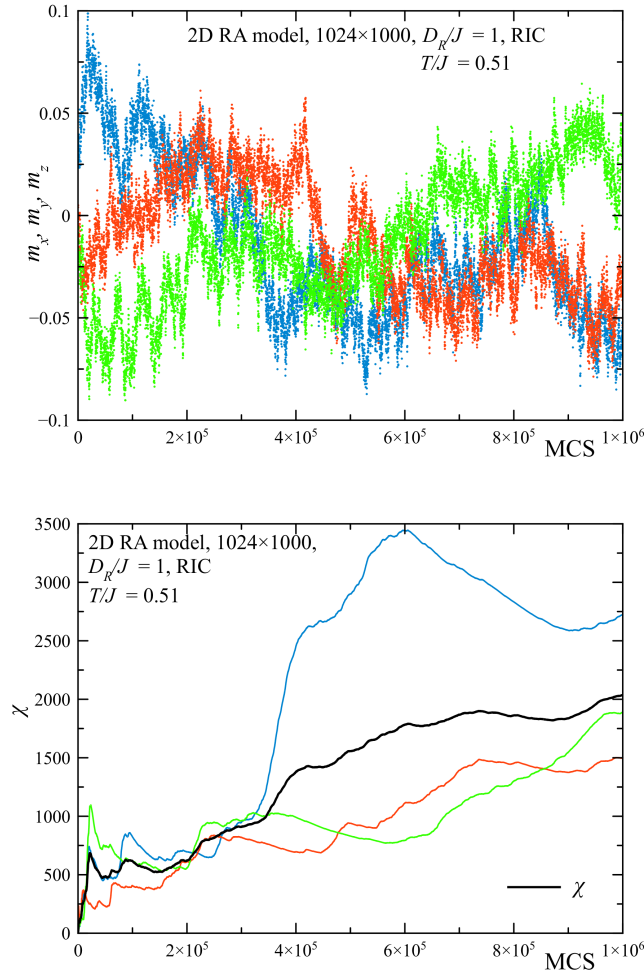


Figure 11: Simulation just below the freezing point,  $T/J = 0.51$ . Upper panel: evolution of the magnetization components. Lower panel: dependence of the susceptibility components (colored curves) and the symmetrized susceptibility (black curve) on the number of MCS done. The system does not come to equilibrium and  $\chi$  does not stabilize with increasing of the number of MCS done.

ing/melting is the fact that in systems with quenched disorder the properties averaged over large regions should fluctuate. If in one region the averaged random anisotropy is larger than in the others, freezing /melting in this region will occur at slightly higher temperatures. Thus the freezing temperature will be spread. At some temperature, most of the system will be melted while some minority regions will be still frozen, providing a small but nonzero value of the spin-glass order parameter  $q$ . In this scenario,  $q(T)$  dependence is neither a power nor an exponential of the temperature.

In the frozen state, as can be seen in Fig. 8, the SG order parameter quickly reaches its asymptotic value that is smaller than one because of the thermal motion of spins on IM domains in their valleys without crossing the barriers

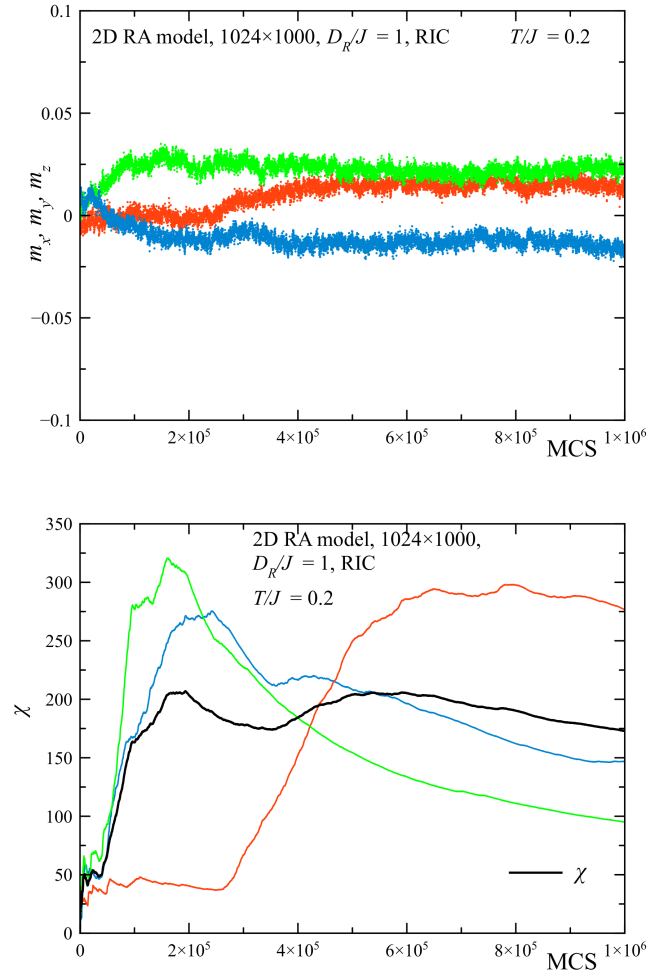


Figure 12: Simulation at a lower temperature,  $T/J = 0.2$ . Upper panel: evolution of the magnetization components; Lower panel: dependence of the susceptibility components (colored curves) and the symmetrized susceptibility (black curve) on the number of MCS done.

ers to different valleys. With increasing the temperature towards the melting point, the processes of crossing the barriers begin and  $q$  slowly decreases. Above the freezing point, such as  $T/J = 0.6$ , the SG order parameter quickly decreases to zero.

The values of the SG order parameter  $q$  computed at different temperatures are shown in Fig. 9. The curve with open circles was obtained by gradually lowering the temperature making  $2 \times 10^4$  MCS for each  $T$  value. This duration of annealing is insufficient to reach stable results. The points of the curve with filled circles obtained one by one for different RA realizations with  $10^6$  MCS are significantly shifted down. In this case, the equilibrium is reached in the main part of the temperature interval except for the vicinity of the freezing transition. This is confirmed by the plateaus of  $q$  vs the number of MCS in Fig. 8.

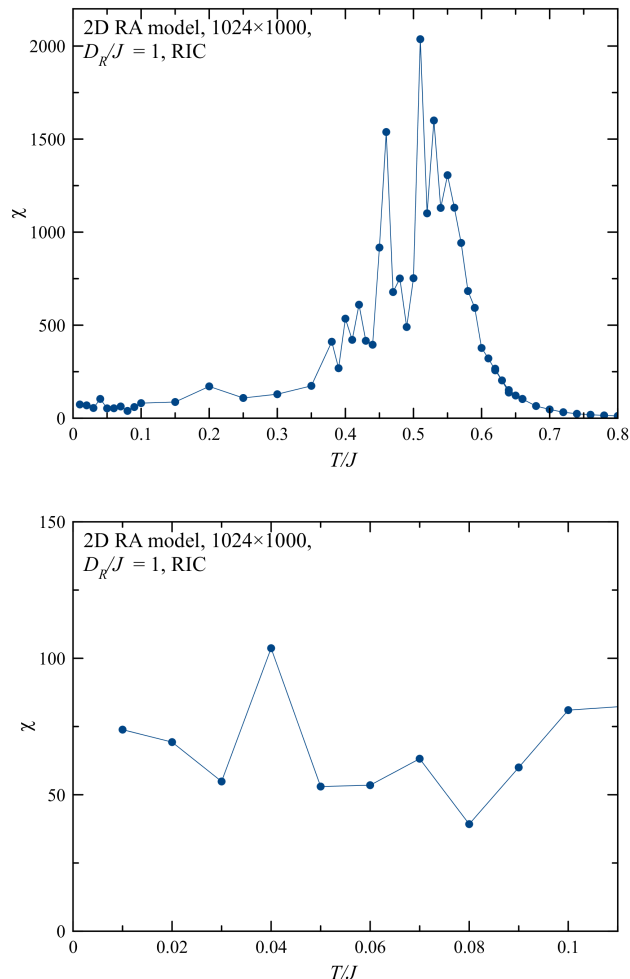


Figure 13: Linear susceptibility  $\chi$  at different temperatures. Upper panel: broad temperature range; Lower panel: Low temperatures.

### C. Magnetization and susceptibility

Above the freezing point, the components of the magnetization defined by Eq. (15) fluctuate fast around zero, as can be seen in the upper panel of Fig. 10. Even for a disordered system of one million spins the magnetization is significant that is the consequence of a strong short-range order that establishes below  $T/J = 0.7$  where the system has the maximum of the heat capacity, even in the absence of the RA. Because of the fast fluctuations, the linear susceptibility computed with the use of Eqs. (19) and (20) and shown in the lower panel of Fig. 10 reaches its asymptotic value within the simulation interval of  $10^6$  MCS. Different components of the susceptibility have approximately the same value.

On the contrast, in the intermediate temperature range at and below freezing, in addition to fast fluctuations of the magnetization, there is slow dynamics, apparently due to thermally-activated barrier crossing. As can be

seen in the upper panel of Fig. 11, slow changes of  $\mathbf{m}$  do not average out within the simulation interval of  $10^6$  MCS. Slow fluctuations of  $\mathbf{m}$  are large and thus make a large contribution to the linear susceptibility. As can be seen in the lower panel of Fig. 11, the susceptibility does not stabilize and continues to grow. In this temperature range, the susceptibility values are huge because of the correlated motion of large groups of spins over energy barriers.

At lower temperatures, there are no large fluctuations of the magnetization due to overbarrier transitions, as can be seen in the upper panel of Fig. 12. The fluctuations seen in the figure are due to the motion of correlated spin bundles within their valleys. Note that  $z$  axis is chosen in the direction of the magnetization in the initial state obtained by the energy minimization from the random spin state.

The values of the symmetrized linear susceptibility  $\chi$  at different temperatures computed using Eq. (20) are shown in Fig. 13. At higher temperatures, the susceptibility is small and practically coincides with that of the pure system. One can see that  $\chi$  has huge values in the region of freezing. However, the values obtained in this region strongly fluctuate and are only approximate as the simulation duration of  $10^6$  MCS proves to be insufficient to average out the magnetization fluctuations (see the upper panel of Fig. 11). Better results, probably, could be obtained for the simulation longer by an order of magnitude that for such a large system is problematic. At low temperatures, the scatter in the susceptibility decreases and the susceptibility values approach a plateau with the height in a fair accordance with Eq. (5) that for  $D_R/J = 1$  with  $R_f/a \approx 13.3$  and  $k = 0.5$  yields  $\chi J \simeq 88$ .

In addition, one could compute the correlation functions (CFs) of the  $\mathbf{m}$  time series shown in figures above. Above freezing, these CFs quickly decay to zero, At intermediate temperatures, they decrease slowly with large fluctuations, as suggested by the upper panel of Fig. 11. At low temperatures where there are no overbarrier transitions, time CFs quickly decrease from their equal-time values to their plateau values. These CFs have been computed for the same model from the dynamical evolution and shown in Fig. 3 of Ref. 39, Those results suggest freezing at  $T/J$  between 0.5 and 0.6, in accordance with the current, more precise, results.

## VII. DISCUSSION

Most of the previous studies of random-anisotropy (RA) magnets were focused on their equilibrium behavior or on their quasi-equilibrium properties in a frozen glassy state. Rigorous analytical solution of this set of problems has never been provided, while numerical studies have been hampered by the necessity to consider large systems in order to account for extended ferromagnetic correlations. Capabilities of modern computers have allowed us to revisit this problem. In this paper we have

studied glassy properties of the random-anisotropy magnet as a function of temperature with the combination of the Metropolis Monte Carlo method and specially developed thermalized overrelaxation.

The questions we asked are the extent to which metastability plays a role in defining magnetic properties of such a system, the freezing of the magnetic configuration due to energy barriers on lowering temperature vs a spin-glass transition due to exchange interaction between spins, the time evolution of a conventionally defined spin-glass order parameter, the characteristic melting time in the temperature region just above freezing, the field-cooled (FC) and zero-field-cooled (ZFC) magnetization curves, and the temperature dependence of the magnetic susceptibility of RA magnets. The computed energy barriers agree within order of magnitude with the Imry-Ma argument for systems with quenched disorder. The computed FC and ZFC magnetization curves have close resemblance with the experimental curves. These findings provide confidence in our numerical method.

A more challenging task has been distinguishing between blocking of overbarrier spin-group transitions on reducing temperature (that implies the Arrhenius temperature dependence of the melting time above freezing) and a true spin-glass phase transition (that implies a power-law divergence of the melting time at transition point). While we cannot say with confidence that we have

answered this question unambiguously, our findings provide a stronger argument in favor of a continuous freezing (blocking) transition on lowering temperature. The main evidence of this is a rather high power in the power-law fit of the melting time and a rather low resulting transition temperature. In accordance with our numerical experiments, the maximum of the susceptibility occurs where the FC and ZFC magnetization curves merge. The low temperature value of the susceptibility roughly agrees with the one derived from the Imry-Ma argument. The temperature dependence of the susceptibility near and below the maximum has a strong scatter caused by the finite size of the system (one million spins) and finite computing time (one million Monte Carlo steps). It did not allow us to distinguish between a smooth behavior at the maximum and a cusp that was experimentally observed in spin glasses. Studies of larger systems and longer computation times would be needed to make such a distinction.

### Acknowledgments

This work has been supported by the Grant No. FA9550-20-1-0299 funded by the Air Force Office of Scientific Research.

- 
- <sup>1</sup> P. Marin and A. Hernando, Applications of amorphous and nanocrystalline magnetic materials, *Journal of Magnetism and Magnetic Materials* **215-216**, 729-734 (2020).
- <sup>2</sup> E. M. Chudnovsky, Random Anisotropy in Amorphous Alloys, Chapter 3 in the Book: *Magnetism of Amorphous Metals and Alloys*, edited by J. A. Fernandez-Baca and W.-Y. Ching, pages 143-174 (World Scientific, Singapore, 1995).
- <sup>3</sup> E. M. Chudnovsky and J. Tejada, *Lectures on Magnetism* (Rinton Press, Princeton, New Jersey, 2006).
- <sup>4</sup> T. C. Proctor, E. M. Chudnovsky, and D. A. Garanin, Scaling of coercivity in a 3d random anisotropy model, *Journal of Magnetism and Magnetic Materials*, **384**, 181-185 (2015).
- <sup>5</sup> D. A. Garanin and E. M. Chudnovsky, Absorption of microwaves by random-anisotropy magnets, *Physical Review B* **103**, 214414-(11) (2021).
- <sup>6</sup> Y. Imry and S.-k. Ma, Random-field instability of the ordered state of continuous symmetry, *Physical Review Letters* **35**, 1399-1401 (1975).
- <sup>7</sup> E. M. Chudnovsky, A theory of two-dimensional amorphous ferromagnet, *Journal of Magnetism and Magnetic Materials* **40**, 21-26 (1983).
- <sup>8</sup> E. Chudnovsky and R. Serota, Correlated spin glass: A new way to extremely soft magnetic materials, *IEEE Transactions on Magnetics* **20**, 1400-1402 (1984).
- <sup>9</sup> E. M. Chudnovsky, W. M. Saslow, and R. A. Serota, Ordering in ferromagnets with random anisotropy, *Physical Review B* **33**, 251-261 (1986).
- <sup>10</sup> R. Seshadri and R.M. Westervelt, Statistical mechanics of magnetic bubble arrays. I. Topology and thermalization, *Physical Review B* **46**, 5142-5149 (1992); *ibid.* II. Observations of two-dimensional melting, **46**, 5150-5161 (1992).
- <sup>11</sup> E. M. Chudnovsky, Hexatic vortex glass in disordered superconductors, *Physical Review B* **40**, 11355-11357 (1989).
- <sup>12</sup> See, e.g., G. Blatter, M. V. Feigel'man, V. B. Geshkenbein, A.I. Larkin, and V. M. Vinokur, Vortices in high-temperature superconductors, *Review of Modern Physics* **66**, 1125-1388 (1994), and references therein.
- <sup>13</sup> K. B. Efetov and A. I. Larkin, Charge-density wave in a random potential, *Soviet Physics JETP* **45**, 1236-1241 (1977).
- <sup>14</sup> J.-i. Okamoto, C. J. Arguello, E. P. Rosenthal, A. N. Pasupathy, and A. J. Millis, Experimental evidence for a bragg glass density wave phase in a transition-metal dichalcogenide, *Physical Review Letters* **114**, 026802-(5) (2015).
- <sup>15</sup> T. C. Proctor and E. M. Chudnovsky, Effect of a dilute random field on a continuous-symmetry order parameter, *Physical Review B* **91**, 140201-(4)R (2015).
- <sup>16</sup> T. Bellini, N. A. Clark, V. Degiorgio, F. Mantegazza, and G. Natale, Light-scattering measurement of the nematic correlation length in a liquid crystal with quenched disorder, *Physical Review E* **57**, 2996-3006 (1998).
- <sup>17</sup> G. E. Volovik, On Larkin-Imry-Ma state in <sup>4</sup>He-A in aerogel, *Journal of Low Temperature Physics* **150**, 453-463 (2008).
- <sup>18</sup> J. I. Li, J. Pollanen, A. M. Zimmerman, C. A. Collett, W. J. Gannon, and W.P. Haperin, The superfluid glass phase of <sup>3</sup>He-A, *Nature Physics* **9**, 775-779 (2013).
- <sup>19</sup> G. E. Volovik, Topology of a <sup>3</sup>He-A film on a corrugated

- graphene substrate, JETP Letters **2107**, 115-118 (2018).
- <sup>20</sup> D. E. Feldman, Quasi-long-range order in the random anisotropy Heisenberg model: Functional renormalization group in  $4 - \epsilon$  dimensions, Physical Review B **61**, 382-390 (2000).
- <sup>21</sup> T. Nattermann and S. Scheidl, Vortex-glass phases in type-II superconductors, Advances in Physics **49**, 607-704 (2000).
- <sup>22</sup> R. A. Serota and P. A. Lee, Continuous-symmetry ferromagnets with random anisotropy, Journal of Applied Physics **61**, 3965-3967 (1987).
- <sup>23</sup> B. Dieny and B. Barbara, XY model with weak random anisotropy in a symmetry-breaking magnetic field, Physical Review B **41**, 11549-11556 (1990).
- <sup>24</sup> R. Dickman and E. M. Chudnovsky, XY chain with random anisotropy: Magnetization law, susceptibility, and correlation functions at  $T = 0$ , Physical Review B **44**, 4397-4405 (1991).
- <sup>25</sup> I. Y. Korenblit and E. F. Shender, Spin glasses and nonergodicity, Soviet Physics Uspekhi **32**, 139-162 (1989).
- <sup>26</sup> D. A. Garanin and E. M. Chudnovsky, Ordered vs. disordered states of the random-field model in three dimensions, European Journal of Physics B **88**, 81-(19) (2015).
- <sup>27</sup> D. A. Garanin, E. M. Chudnovsky, and T. Proctor, Random field xy model in three dimensions, Physical Review B **88**, 224418-(21) (2013).
- <sup>28</sup> T. C. Proctor, D. A. Garanin, and E. M. Chudnovsky, Random fields, Topology, and Imry-Ma argument, Physical Review Letters **112**, 097201-(4) (2014).
- <sup>29</sup> E. M. Chudnovsky and D. A. Garanin, Topological order generated by a random field in a 2D exchange model, Physical Review Letters **121**, 017201-(4) (2018).
- <sup>30</sup> R. Fisch, Random field and random anisotropy effects in defect-free three-dimensional XY models, Physical Review B **62**, 361-366 (2000).
- <sup>31</sup> M. Itakura, Frozen quasi-long-range order in the random anisotropy Heisenberg magnet, Physical Review B **68**, 100405-(4) (R) (2003).
- <sup>32</sup> D. Imagawa and H. Kawamura, Monte Carlo study of the ordering of the weakly anisotropic Heisenberg spin glass in magnetic fields, Physical Review B **70**, 144412-(16) (2004).
- <sup>33</sup> M. Dudka, R. Folk, and Y. Holovatch, Critical properties of random anisotropy magnets, Journal of Magnetism and Magnetic Materials **294**, 305-229 (2005).
- <sup>34</sup> K. Binder and A. P. Young, Spin glasses: Experimental facts, theoretical concepts, and open questions, Review of Modern Physics **58**, 801-976 (1986).
- <sup>35</sup> O. V. Billoni, S. A. Cannas, and F. A. Tamarit, Spin-glass behavior in the random-anisotropy Heisenberg model, Physical Review B **72**, 104407-(4) (2005).
- <sup>36</sup> P. M. Shand, C. C. Stark, D. Williams, M. A. Morales, T. M. Pekarek, and D. L. Leslie-Pelecky, Spin glass or random anisotropy?: The origin of magnetically glassy behavior in nanostructured  $\text{GdAl}_2$ , Journal of Applied Physics **97**, 10J505-(3) (2005).
- <sup>37</sup> D. A. Garanin, Energy balance and energy correction in dynamics of classical spin systems, Physical Review E **104**, 055306-(8) (2021).
- <sup>38</sup> W. B. Nurdin and K.-D. Schotte, Dynamical temperature for spin systems, Physical Review E **61**, 3579-3582 (2000).
- <sup>39</sup> D. A. Garanin and E. M. Chudnovsky, Nonlinear and Thermal Effects in the Absorption of Microwaves by Random Magnets, arXiv:2108.09804